

# Self-assembly of a sulphur-terminated graphene nanoribbon within a single-walled carbon nanotube

A. Chuvilin<sup>1,2</sup>, E. Bichoutskaia<sup>3</sup>, M. C. Gimenez-Lopez<sup>3</sup>, T. W. Chamberlain<sup>3</sup>, G. A. Rance<sup>3</sup>, N. Kuganathan<sup>3</sup>, J. Biskupek<sup>4</sup>, U. Kaiser<sup>4</sup> and A. N. Khlobystov<sup>3\*</sup>

**The ability to tune the properties of graphene nanoribbons (GNRs) through modification of the nanoribbon's width and edge structure<sup>1–3</sup> widens the potential applications of graphene in electronic devices<sup>4–6</sup>. Although assembly of GNRs has been recently possible, current methods suffer from limited control of their atomic structure<sup>7–13</sup>, or require the careful organization of precursors on atomically flat surfaces under ultra-high vacuum conditions<sup>14</sup>. Here we demonstrate that a GNR can self-assemble from a random mixture of molecular precursors within a single-walled carbon nanotube, which ensures propagation of the nanoribbon in one dimension and determines its width. The sulphur-terminated dangling bonds of the GNR make these otherwise unstable nanoribbons thermodynamically viable over other forms of carbon. Electron microscopy reveals elliptical distortion of the nanotube, as well as helical twist and screw-like motion of the nanoribbon. These effects suggest novel ways of controlling the properties of these nanomaterials, such as the electronic band gap and the concentration of charge carriers.**

Single-walled carbon nanotubes (SWNTs) with typical diameters of 0.7–2.0 nm are ideal containers for medium-sized molecules. Carbon cages of fullerenes, having a particularly strong affinity for the interiors of nanotubes, have been studied within nanotubes more than any other molecular species<sup>15</sup>. Triggered by heat or electron beam (e-beam) radiation, fullerenes undergo chemical transformations in SWNTs. Although the nanotube itself is not involved in the reactions of the guest-molecules, it imposes severe limitations on the structure of the product formed<sup>16</sup>. For example, fullerene epoxide (C<sub>60</sub>O) forms strictly linear polymer chains within a SWNT, whereas the same reaction taking place outside the nanotube leads to the formation of branched, highly convoluted polymers<sup>16</sup>. This clearly illustrates the unique ability of nanotubes to act not only as containers, but also as efficient templates for the synthesis of structures that otherwise would not exist.

Under harsh heating (>800 °C) or e-beam irradiation conditions more drastic transformations of molecules can also take place inside nanotubes. Fullerenes, for example, break down into small clusters of atoms and transform into a narrow nanotube nestled within the original host-SWNT, producing a SWNT@SWNT system<sup>17</sup>. Once again, the host-nanotube acts as a template that prevents the formation of the thermodynamically most stable form of carbon (namely graphite) by restricting the growth in two dimensions, leading to the formation of a 1D structure

(namely the guest-SWNT). In principle, the 1D structure of a carbon nanoribbon is also compatible with the geometry of the host-SWNT, but in practice the growth of GNRs has never been observed in nanotubes. Our calculations of the Gibbs free energy of formation (per atom)  $\delta G$  for various 1D nanostructures clearly indicate that a guest-SWNT is significantly more stable than a GNR of a similar width (Fig. 1 and Supplementary Table S1), despite the fact that the bond lengths and angles of the latter are closer to the ideal geometry of an  $sp^2$ -carbon atom. The key reason for the lower stability of GNRs is related to the unsaturated valences of the carbon atoms at the edge of the nanoribbon, which have only two bonds instead of the three that are required for an  $sp^2$ -carbon atom. However, interestingly, once the edges of the nanoribbon are terminated with heteroatoms (for example H or other non-carbon elements), the resultant edge-terminated GNR becomes thermodynamically more stable than a SWNT (Fig. 1). These simple structural and energetic considerations give an explanation why GNRs cannot be formed from fullerenes and, most importantly, provide a key recipe for the construction of nanoribbons in nanotubes: the growth of stable GNRs requires plenty of carbon—a building element of the GNR itself, as well as some non-carbon elements able to terminate all the edges of the GNR.

The carbon cages of fullerenes possess a rich chemical reactivity that allows the grafting of organic functional groups to the fullerene surface. Thus functionalized fullerenes still retain their exceptional affinity for the interior of the SWNT (refs 18,19), and therefore can be used as shuttles to transport effectively any elements forming the functional group into the nanotube (Fig. 2). The presence of non-carbon elements in the nano-container widens the range of chemical transformations that could take place within the host-SWNT and offers a mechanism for terminating the edges of a nanoribbon. To test this hypothesis, we have designed a complex functional group consisting of a pyrrolidine ring linked to a phenyl ester moiety bearing an alkyl chain with a dithiolane group (Fig. 2a). In addition to 80 atoms of carbon forming the fullerene cage, this molecule contains a selection of hetero-elements H, O, N and S—any of which, in principle, are able to terminate the edge of the GNR (the chemical reactivity of Sc atoms does not allow them to terminate the edges of the GNR). Time series of aberration-corrected high resolution transmission electron microscopy (AC-HRTEM) images reveal that the functional groups of these molecules become fragmented by the 80 keV electron

<sup>1</sup>CIC nanoGUNE Consolider, Tolosa Hiribidea 76, E-20018, Donostia-San Sebastian, Spain, <sup>2</sup>IKERBASQUE, Basque Foundation for Science, 48011 Bilbao, Spain, <sup>3</sup>School of Chemistry, University of Nottingham, University Park, Nottingham NG7 2RD, UK, <sup>4</sup>Central Facility of Electron Microscopy, Group of Electron Microscopy of Materials Science, Ulm University, Albert-Einstein-Allee 11, D-89081 Ulm, Germany. \*e-mail: andrei.khlobystov@nottingham.ac.uk

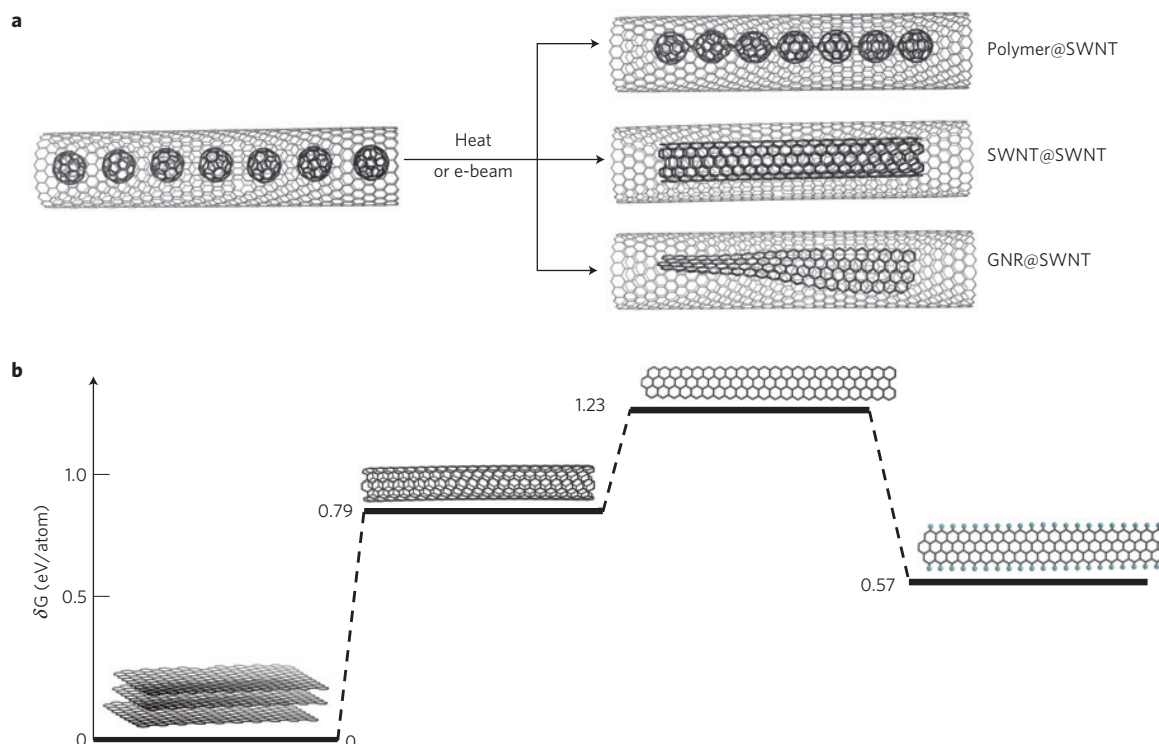


**Figure 1 | Guest-molecules encapsulated within a carbon nanotube can be transformed into a 1D structure under the influence of heat or an electron beam.** **a**, The host-SWNT acts as a template that allows the growth only in one direction. Depending on the conditions, the molecules of fullerene can either be transformed into a polymer (polymer@SWNT) or into a narrow internal nanotube (SWNT@SWNT); although the formation of a nanoribbon within a SWNT is also possible in theory, GNR@SWNT have never been previously observed. **b**, Comparison of the Gibbs free energy ( $\delta G$ ) for different carbon nanostructures clearly shows that a narrow SWNT (0.79 eV/atom) is more thermodynamically stable than a nanoribbon (1.23 eV/atom). The decrease in stability predicted for a GNR is due to the dangling bonds along its edges. Once the edges are terminated with H, S or other non-carbon elements (that is, all dangling bonds are saturated), the terminated nanoribbon becomes more stable (0.57 eV/atom) than a SWNT.

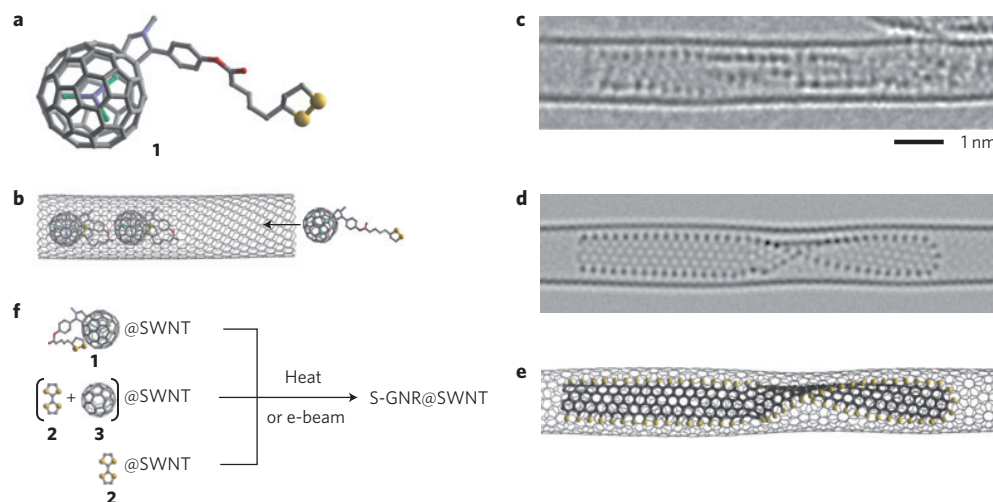


**Figure 2 | Carbon nanotubes serve as containers and nanoreactors for molecules.** Functionalized fullerenes **1** (**a**) bearing an organic group with sulphur atoms on their surface are spontaneously and irreversibly encapsulated into a SWNT (**b**) owing to the strong van der Waals interactions between the fullerene cage and the interior of the host-nanotube. Under prolonged exposure to the e-beam, the functional groups and the fullerene cages decompose and re-assemble into a nanoribbon inside a (14, 5)-SWNT (**c**). Sulphur atoms terminating the edges of the nanoribbon appear as chains of dark atoms (**c**, an experimental AC-HRTEM image, **e**, a model of S-GNR@SWNT and **d**, an image simulated from the model). Sulphur-terminated nanoribbons can also be formed from other sulphur-containing organic molecules, such as TTF **2** or a mixture of TTF **2** and C<sub>60</sub> **3** inserted in nanotubes (**f**) at high temperature (1,000 °C) or under e-beam radiation. (In the structural diagrams atoms of sulphur, oxygen, nitrogen and carbon are coloured in yellow, red, blue and grey respectively; atoms of hydrogen in the structural diagram of **1** are omitted for clarity.)

1 beam<sup>20</sup>, followed by breakage of the fullerene cages themselves  
 2 (Supplementary Fig. S1), thus forming a dynamic mixture of several  
 3 chemical elements within the cavity of the host-nanotube.

Under prolonged exposure to the e-beam, molecules containing  
 4 no elements that could saturate the valences of  $sp^2$ -carbon (for  
 5 example C<sub>60</sub>, M@C<sub>82</sub>) invariably convert into a guest-SWNT  
 6

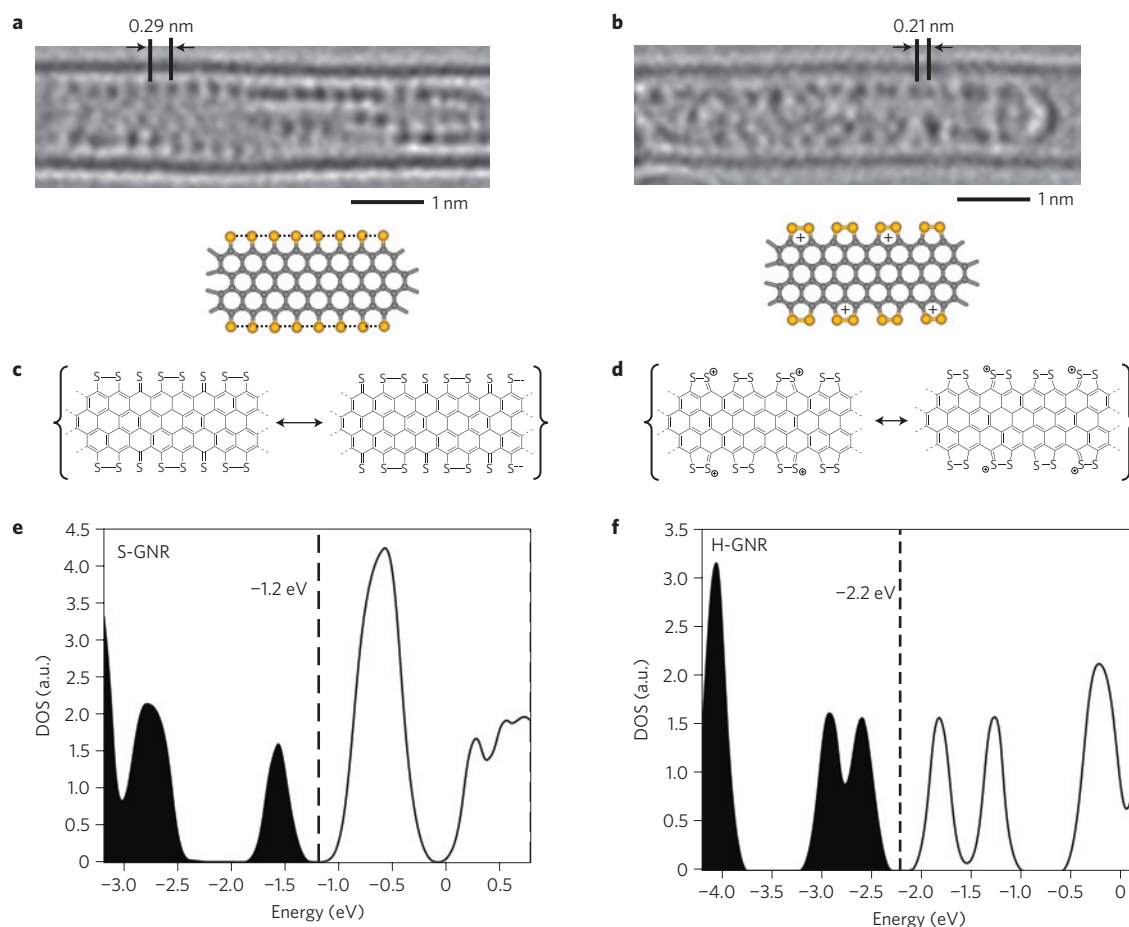


**Figure 3 | Structure and properties of sulphur-terminated nanoribbon.** At the beginning of the exposure to the e-beam, the sulphur atoms at the edge of the nanoribbon are equidistantly spaced by 0.29 nm (a), indicating weak bonding between the neighbouring atoms (the bond order of the S-S bond is less than one; c—some resonance forms of the S-GNR). Extensive irradiation with the e-beam removes some of the valence electrons and ‘oxidizes’ the S-GNR (b) causing formation of dithiolium pentagonal rings where the S-S bond has an order of one (d—some resonance forms of  $[S\text{-GNR}]^{n+}$ ). As a result, the sulphur atoms are observed in pairs. The density of states calculated for S-GNR (e) and H-GNR (f) illustrate that termination of the GNR with sulphur atoms maintains the semiconducting character of the nanoribbon but substantially shifts its Fermi level (indicated by a dashed line), thus making the nanoribbon more electron donating. States populated with electrons and empty states are shown as black and white bands respectively.

1 (Fig. 1a; refs 21,22). However, the functionalized fullerene under  
 2 similar conditions forms a completely different structure, consisting  
 3 of two chains of dark atoms running parallel to each other (Fig. 2c).  
 4 A close inspection of the space between the chains reveals three  
 5 rows of fused hexagonal rings, equivalent to those in graphene  
 6 (Fig. 2c). As only sulphur has an atomic number high enough  
 7 ( $Z = 16$ ) to account for the observed dark atoms (the single-atom  
 8 contrast of N and O will be much lower and indistinguishable  
 9 from that of C)<sup>23</sup>, these observations are consistent with a zigzag  
 10 nanoribbon with edges that are terminated by sulphur atoms  
 11 (S-GNR, Figs 2e, 3a, Supplementary Video S1). In the presence  
 12 of a plentiful supply of other elements (H, N, O) termination  
 13 with sulphur is fairly unexpected. However, considering that the  
 14 nanoribbon is formed under a continuous bombardment of the  
 15 e-beam, sulphur atoms are least likely to be removed owing to  
 16 the collisions with electrons, as the energy transferred from the  
 17 e-beam to the atom is inversely proportional to its atomic number<sup>24</sup>.  
 18 Therefore, lighter elements (N, O and particularly H) would be  
 19 stripped away by the e-beam very quickly, making them less suitable  
 20 for the termination of GNRs.

21 The selective affinity of the nanoribbon for sulphur atoms was  
 22 confirmed by the observation that GNRs can be readily formed  
 23 from a mixture of  $C_{60}$  and tetrathiafulvalene (TTF, a sulphur rich  
 24 molecule with the formula  $C_6H_4S_4$ ) or even from tetrathiafulvalene

itself inserted in SWNT (Fig. 2f and Supplementary Figs S2–S4 and  
 Video S2). The observed nanoribbons were up to 20 nm in length,  
 and energy dispersive X-ray (EDX) spectroscopy confirmed the  
 nature of the atoms terminating their edges as sulphur (Supple-  
 mentary Fig. S3). Most importantly, the formation of S-GNR was  
 shown to be triggered by heat as well as by e-beam radiation, thus  
 giving a route for the mass production of these nanostructures.  
 Raman spectroscopy (recorded using a green laser at  $\lambda_{\text{ex}} = 538$  nm)  
 shows that the vibrational bands of TTF@SWNT at  $\sim 1,420$   $\text{cm}^{-1}$   
 and  $490$   $\text{cm}^{-1}$ , corresponding to a C=C stretch and pentagonal ring  
 bend respectively, after heating at  $1,000$   $^{\circ}\text{C}$  become replaced by a  
 C=S bond stretch at  $\sim 1,200$   $\text{cm}^{-1}$  of the nanoribbon edge (the  
 vibrations of the carbon–carbon bonds of the S-GNR are obscured  
 by the Raman bands of the SWNT; Supplementary Fig. S5). These  
 examples illustrate that the formation of GNRs is a spontaneous  
 self-assembly process that can take place from a random mixture  
 of atoms (as long as it contains C and S), regardless of the actual  
 structure of the molecular precursors and their elemental composition.  
 We were not able to observe the actual mechanism of the nanorib-  
 bon formation from functionalized fullerenes or from TTF in direct  
 space by AC-HRTEM, partly because the reactive intermediates  
 move within the host-SWNT on a timescale much faster than the  
 image capture rate (approximately 1 s). However, considering that  
 the formation of S-GNR requires either irradiation with accelerated

25  
26  
27  
28  
29  
30  
31  
32  
33  
34  
35  
36  
37  
38  
39  
40  
41  
42  
43  
44  
45  
46  
47  
48

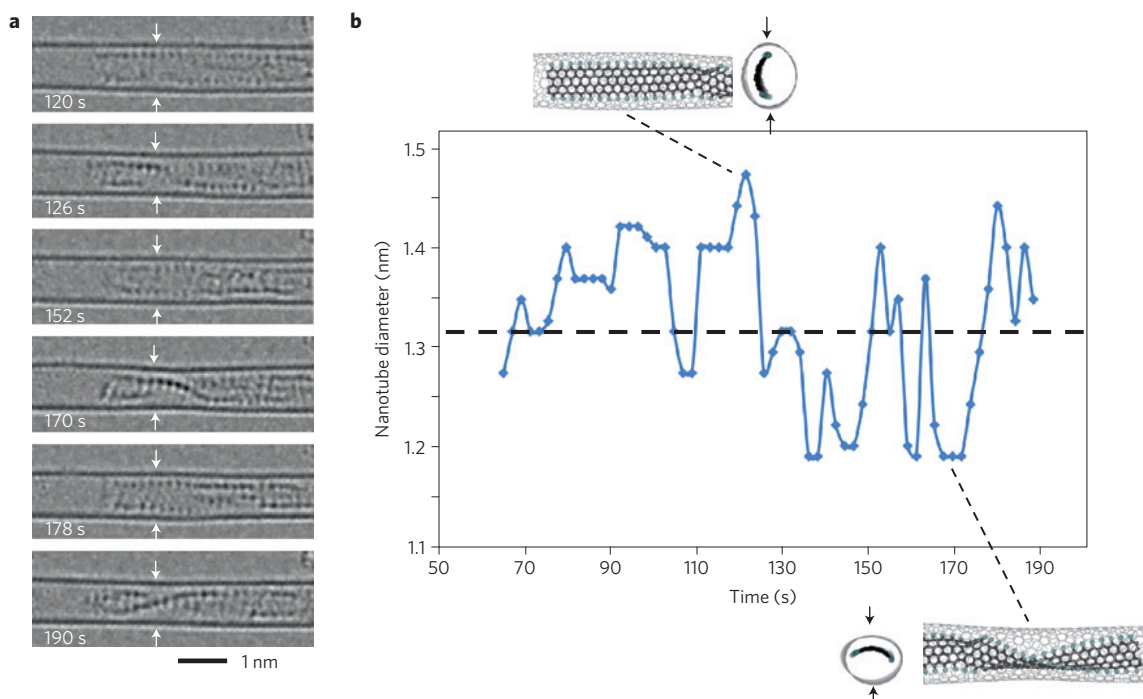


**Figure 4 | Dynamic behaviour of the nanoribbon inside the nanotube. a**, A time series of images showing rotation of the S-GNR inside a carbon nanotube. The cross-section of the host-nanotube is elliptically distorted by the guest-nanoribbon: the nanotube is stretched within the plane of the S-GNR and contracted in the orthogonal plane. The projection of the nanotube diameter is measured for each image along the line designated by the two white arrows and **(b)** plotted as a function of time (dashed line indicates the nominal diameter of a cylindrical, undistorted (14, 5)-SWNT).

1 electrons or heating at very high temperature and is independent of  
 2 the structure of the molecular precursors, the nanoribbon is likely  
 3 to be formed from C<sub>2</sub> fragments and atomic sulphur generated from  
 4 molecules broken down under these harsh conditions.

5 Sulphur atoms can bind to the edges of a zigzag nanoribbon  
 6 using several different modes. AC-HRTEM imaging narrows  
 7 down the possible options by revealing two important structural  
 8 features of S-GNRs: the sulphur atoms are positioned directly  
 9 opposite each other across the nanoribbon width and are spaced  
 10 equidistantly by ~0.29 nm along the nanoribbon edge (Fig. 3a).  
 11 Considering that the S-GNR consists of three rows of hexagons,  
 12 it is structurally related to peripentacene<sup>25,26</sup> and can be formally  
 13 classified as a polythiaperipolycene. As such, the S-GNR possesses  
 14 many resonance forms that would merge into a superposition  
 15 (Fig. 3c). As a result, all S–S distances along the nanoribbon edge  
 16 will be of the same length, corresponding to a bond order of less  
 17 than one<sup>27</sup>, which is consistent with the AC-HRTEM observations.  
 18 Importantly, towards the end of the AC-HRTEM time series the  
 19 equidistant separation between the sulphur atoms changes to an  
 20 alternating pattern of long (~0.34 nm) and short (~0.21 nm)  
 21 S–S distances, which indicates a change in the bonding between  
 22 the terminal atoms of the S-GNR induced by exposure to the  
 23 e-beam (Fig. 3b). As the incident e-beam gradually removes valence  
 24 electrons from the S-GNR (in chemical terms, the e-beam can be  
 25 viewed as an oxidant) the pentagonal rings at the edges of the  
 26 S-GNR turn into dithiolium cations (Fig. 3d), which are known to  
 27 be very stable. In the presence of the cationic dithiolium groups,  
 28 the equidistant separation of S-atoms is no longer possible, as the  
 29 resonance forms with S-atoms sitting in pairs within the dithiolium  
 30 cation rings become predominant. The length of the S–S bond in  
 31 dithiolium cations is known to be 0.21 nm (ref. 27), which is in  
 32 agreement with the AC-HRTEM measurements.

33 The lengths of the nanoribbons observed in our experiments  
 34 are in the range of 7–28 nm. However, it should be noted that the  
 35 length measurements are limited by the field of view of HRTEM,

36 because there is no fundamental reason why nanoribbons cannot be  
 37 formed throughout the entire length of the host-nanotube, resulting  
 38 in S-GNRs up to several micrometres long.

39 Owing to the fact that carbon atoms at the edges of the GNR  
 40 have very different bonding characteristics to carbon atoms in the  
 41 middle of the nanoribbon, zigzag GNRs are predicted to exhibit very  
 42 unusual electron transport and magnetic properties<sup>28–30</sup>. Our spin-  
 43 unrestricted density functional theory (DFT) calculations show  
 44 that a S-GNR has a nonzero direct band gap of 0.5 eV, which is  
 45 similar in value to that of the H-terminated zigzag nanoribbons  
 46 (H-GNR) (Fig. 3e,f). The electronic band gap in a zigzag GNR  
 47 can be controlled by an applied electric field<sup>29,30</sup>, which opens  
 48 up possibilities for the applications of GNRs in spintronics. Edge  
 49 termination with sulphur atoms significantly lifts the energy of  
 50 the Fermi level in S-GNR to –1.2 eV, as compared with –2.2 eV  
 51 in H-GNR. Thus, a S-GNR is expected to possess strong electron  
 52 donating properties, which may lead to substantial electron transfer  
 53 from the guest-nanoribbon to the host-nanotube (the typical Fermi  
 54 level energy in the SWNT is –4.5 eV).

55 Our calculations show that the van der Waals width of the  
 56 S-GNR exceeds the nominal diameter of the (14, 5) host-nanotube  
 57 (1.32 nm), such that it would not be possible to insert a perfectly  
 58 flat nanoribbon into a perfectly cylindrical nanotube. We have  
 59 identified two mechanisms that allow for the nanoribbon to  
 60 be accommodated within the nanotube. The first mechanism is  
 61 the distortion of the SWNT cross-section into an elliptic shape  
 62 (Fig. 4b). As the nanoribbon rotates inside the nanotube the  
 63 nanotube seems to be expanding within the plane of the S-GNR and  
 64 contracting in the orthogonal direction (also see Supplementary  
 65 Videos S1 and S3). The measured variation in the projected width  
 66 of the host-nanotube is 0.25 nm, which corresponds to about 20%  
 67 of the SWNT diameter and, therefore, imposes significant strain on  
 68 the nanotube sidewall. The second mechanism is a spiral distortion  
 69 of the nanoribbon itself (Fig. 4), which is a rather surprising result  
 70 as nanoribbons synthesized outside the nanotubes are typically



considered as flat, linear structures. Our time series AC-HRTEM imaging clearly demonstrates that the nanoribbon is a soft, flexible structure that can readily adopt a helical conformation, slightly resembling the shape of a party streamer. The spiral shape reduces the effective width of the S-GNR and potentially enables van der Waals interactions with the interior walls of the host-SWNT, which may additionally stabilize the S-GNR@SWNT structure. Notably, throughout the observation, the S-GNR remains mobile and rotates axially within the nanotube, thus indicating no chemical bonding between the nanoribbon and the nanotube container.

A previous theoretical study described non-planar configurations for narrow nanoribbons with unterminated edges (that is, containing highly unstable dangling bonds) predicting a ‘saddle-shape chain’ and a ‘double helix’ for these hypothetical GNRs (ref. 31). However, on the edge termination with H atoms, all the nanoribbons were predicted to adopt a strictly flat shape. In our case, the experimentally observed ‘party streamer’ helical conformation of the GNR is qualitatively different to the predicted shapes<sup>31</sup> and is largely controlled by the confinement within the host-nanotube (similar to the atomic chains of iodine<sup>32</sup> or supramolecular chains of fullerenes<sup>19</sup> spontaneously forming helical arrangements in nanotubes of certain diameters). The helical twist of the nanoribbon can be a key parameter in determining the electromechanical properties of the GNRs, as their electronic band gaps are predicted to be critically dependent on the twist angle<sup>33</sup>. This could give rise to interesting piezoelectric effects at the nanoscale, as compression of the nanotube would result in changes in the electric properties of the GNR and vice versa.

This study outlines a new strategy for spontaneous self-assembly of GNRs with well-defined atomic structure from a mixture of atoms, using a SWNT as both the reaction vessel and template for nanoribbon growth, and presents the first example of GNR@SWNT—a new hybrid form of carbon nanomaterial. We identify the two key principles that lead to the formation of GNR: (1) 1D confinement at the nanoscale ensures propagation of the GNR in only one dimension, and (2) incorporation of heteroatoms into the predominantly carbon-based elemental feedstock leads to the termination of dangling bonds, stabilizing the structure. The surprising termination of nanoribbons with sulphur atoms may open avenues that have not been considered so far, even theoretically. The semiconducting properties of S-GNRs and the complex dynamic behaviour of the nanoribbon inside the nanotube (rotation and translation) observed in our study may pave the way for future applications of these materials in electronic and mechanical nanodevices. This new form of nanomaterial, where a 1D nanostructure is encapsulated within another 1D nanostructure, is likely to stimulate a new wave of experimental and theoretical studies.

## Methods

**Synthesis of functionalized fullerene and its insertion into SWNTs.** Details of the synthesis of *N*-methyl-2-(4-(liponyloxy)benzyl)-[5,6]-Sc<sub>3</sub>N@C<sub>60</sub> fulleropyrrolidine **1** are in the Supplementary Synthetic Methods. The structure of **1** was verified by spectroscopy before insertion into the nanotubes: MALDI-MS 1447.14 *m/z* [M]<sup>-</sup>. <sup>1</sup>H NMR (500 MHz, CDCl<sub>3</sub>:CS<sub>2</sub> (1:6), 300 K) δ<sub>H</sub> 4.38 (*d*, *J* = 9.7 Hz, 1H, —CH<sub>2</sub> pyrrolidine), 3.76 (s, 1H, —CH pyrrolidine), 3.15 (s, 3H, —NCH<sub>3</sub>), 3.08 (*d*, *J* = 9.7 Hz, 1H, —CH<sub>2</sub> pyrrolidine) ppm. Heteronuclear Multiple Quantum Correlation (HMQC) (500 MHz, CDCl<sub>3</sub>:CS<sub>2</sub> (1:6), 300 K) δ<sub>C</sub> 85.0 (—CH<sub>2</sub> pyrrolidine), 72.5 (—CH pyrrolidine), 41.4 (—NCH<sub>3</sub>) ppm.

Compound **1** was inserted into nanotubes at room temperature from supersaturated chloroform solution (details are in the Supplementary Methods).

**C<sub>60</sub>/TTF@SWNT and TTF@SWNT preparation.** Freshly annealed SWNTs (5 mg, NanoCarbLab, arc discharge) were added immediately to a mixture of tetrathiafulvalene (20 mg) and C<sub>60</sub> (5 mg) at 150 °C under an argon atmosphere. The suspension was stirred for 3 h, allowed to cool, diluted with tetrahydrofuran (2 ml) and filtered onto a PTFE filtration membrane (pore size 0.5 μm). The material was then washed successively with tetrahydrofuran (10 ml) and methanol (10 ml) and dried in air. The process was repeated without the addition of C<sub>60</sub> to yield a sample of TTF@SWNT.

**Thermally activated formation of S-GNR.** Samples of TTF@SWNT were sealed in three quartz tubes under a reduced pressure of argon (680 mbar). Each tube was heated at a different temperature; 250, 600 and 1,000 °C for 20 min, cooled to room temperature and opened. The products were mounted onto Si(100) supports and their Raman spectra were recorded at room temperature (HoribaJY LabRAM HR spectrometer, laser wavelength 532 nm). Only the sample heated at 1,000 °C indicated transformation of TTF into S-GNR (Supplementary Fig. S5) as Raman spectra of all samples heated at lower temperatures remained unchanged.

**80 kV AC-HRTEM measurements.** TEM investigation was performed on a Titan 80-300 (FEI, Netherlands) instrument equipped with an imaging-side aberration corrector. The instrument was operated at 80 kV accelerating voltage. To decrease the influence of the chromatic aberration, which is the limiting factor on resolution at 80 kV, the extractor voltage of the electron gun was decreased to approximately 2,000 V, resulting in a better beam monochromaticity. The coefficient of the spherical aberration, Cs, of the objective lens was set to approximately +20 μm and a defocus of −13 nm was used (slightly below Scherzer defocus) to increase the contrast. The images were zero-loss filtered using a GIF Tridiem (Gatan, USA) and acquired by a Gatan Ultrascan 2K × 2K CCD camera. The exposition time was 1 s, with approximately 2 s intervals between images for time series. Hardware binning × 2 was used for a faster frame rate and to suppress the influence of the modulation transfer function (MTF) of the camera. Significant oversampling (0.023 nm/pix) was used to suppress further the influence of the MTF.

Details of image processing and image simulations are described in the Supplementary Methods and Figs S6 and S7.

Received 21 February 2011; accepted 27 June 2011; published online XX Month XXXX

## References

- Berger, C. *et al.* Electronic confinement and coherence in patterned epitaxial graphene. *Science* **312**, 1191–1195 (2006).
- Son, Y.-W., Cohen, M. L. & Louie, S. G. Half-metallic graphene nanoribbons. *Nature* **444**, 347–349 (2006).
- White, C. T. & Areshkin, D. A. Building blocks for integrated graphene circuits. *Nano Lett.* **7**, 825–830 (2007).
- Yang, L., Cheol-Hwan, P., Son, Y.-W., Cohen, M. L. & Louie, S. G. Quasiparticle energies and band gaps in graphene nanoribbons. *Phys. Rev. Lett.* **99**, 186801 (2007).
- Wakabayashi, K. Electronic transport properties of nanographite ribbon junctions. *Phys. Rev. B* **64**, 125428 (2001).
- Barone, V., Hod, O. & Scuseria, G. E. Electronic structure and stability of semiconducting graphene nanoribbons. *Nano Lett.* **6**, 2748–2754 (2006).
- Datta, S. S., Strachan, D. R., Khamis, S. M. & Jonson, A. T. Crystallographic etching of few-layer graphene. *Nano Lett.* **8**, 1912–1915 (2008).
- Li, X., Wang, X., Zhang, L., Lee, S. & Dai, H. Chemically derived, ultrasmooth graphene nanoribbon semiconductors. *Science* **319**, 1229–1232 (2008).
- Kosynkin, D. V. *et al.* Longitudinal unzipping of carbon nanotubes to form graphene nanoribbons. *Nature* **458**, 872–875 (2009).
- Jiao, L. Y., Zhang, L., Wang, X., Diankov, G. & Dai, H. Narrow graphene nanoribbons from carbon nanotubes. *Nature* **458**, 877–880 (2009).
- Elias, A. L. *et al.* Longitudinal cutting of pure and doped carbon nanotubes to form graphitic nanoribbons using metal clusters as nanoscissors. *Nano Lett.* **10**, 366–372 (2009).
- Yang, X. Y. *et al.* Two-dimensional graphene nanoribbons. *J. Am. Chem. Soc.* **130**, 4216–4217 (2008).
- Jiao, L., Wang, X., Diankov, G., Wang, H. & Dai, H. Facile synthesis of high-quality graphene nanoribbons. *Nature Nanotechnol.* **5**, 321–325 (2010).
- Cai, J. *et al.* Atomically precise bottom-up fabrication of graphene nanoribbons. *Nature* **466**, 470–473 (2010).
- Basiuk, V. A. & Basiuk, E. V. *Chemistry of Carbon Nanotubes*, Vol. 3, Chapter 5 (American Scientific Publishers, 2003).
- Britz, D. A., Khlobystov, A. N., Porfyriakis, K., Ardavan, A. & Briggs, A. D. Chemical reactions inside single-walled carbon test-tubes. *Chem. Commun.* 37–39 (2005).
- Bandow, S., Takizawa, M., Hirahara, K., Yudasaka, M. & Iijima, S. Raman scattering study of double-wall carbon nanotubes derived from the chains of fullerenes in single-wall carbon nanotubes. *Chem. Phys. Lett.* **337**, 48–54 (2001).
- Britz, D. A. *et al.* Selective host–guest interaction of single-walled carbon nanotubes with functionalised fullerenes. *Chem. Commun.* 176–177 (2004).
- Chamberlain, T. W. *et al.* Toward controlled spacing in one-dimensional molecular chains: Alkyl-chain-functionalized fullerenes in carbon nanotubes. *J. Am. Chem. Soc.* **129**, 8609–8614 (2007).
- Gimenez-Lopez, M. C., Chuvilín, A., Kaiser, U. & Khlobystov, A. N. Functionalised endohedral fullerenes in single-walled carbon nanotubes. *Chem. Commun.* doi:10.1039/c0cc02929g (2011).
- Koshino, M. *et al.* Analysis of the reactivity and selectivity of fullerenes dimerization reactions at the atomic level. *Nature Chem.* **2**, 117–124 (2010).

- 1 22. Terrones, M. Electron microscopy: Visualizing fullerene chemistry. *Nature*  
2 *Chem.* **2**, 82–83 (2010).
- 3 23. Meyer, J. C. *et al.* Experimental analysis of charge redistribution due to  
4 chemical bonding by high-resolution transmission electron microscopy.  
5 *Nature Mater.* **10**, 209–215 (2011).
- 6 24. Williams, D. B. & Carter, C. B. *Transmission Electron Microscopy: A Textbook*  
7 *for Materials Science* (Plenum, 1996).
- 8 25. Goodings, E. P., Mitchard, D. A. & Owen, G. Synthesis, structure, and  
9 electrical properties of naphthacene, pentacene, and hexacene sulphides.  
10 *J. Chem. Soc. Perkin Trans.* 1310–1314 (1972).
- 11 26. Briseno, A. L. *et al.* Hexathiapentacene: Structure, molecular packing, and  
12 thin-film transistors. *J. Am. Chem. Soc.* **128**, 15576–15577 (2006).
- 13 27. Klingsberg, E. Thiothiophene no-bond resonance compounds. *Quart. Rev.*  
14 **23**, 537–551 (1969).
- 15 28. Son, Y.-W., Cohen, M. L. & Louie, S. G. Energy gaps in graphene nanoribbon.  
16 *Phys. Rev. Lett.* **97**, 216803 (2006).
- 17 29. Rudberg, E., Salek, P. & Luo, Y. Nonlocal exchange interaction removes  
18 half-metallicity in graphene nanoribbons. *Nano Lett.* **7**, 2211–2213 (2007).
- 19 30. Hod, O., Barone, V., Peralta, J. E. & Scuseria, G. E. Enhanced half-metallicity in  
20 edge-oxidised zigzag graphene nanoribbons. *Nano Lett.* **7**, 2295–2299 (2007).
- 21 31. Bets, K. V. & Yakobson, B. I. Spontaneous twist and intrinsic instabilities of  
22 pristine graphene nanoribbons. *Nano Res.* **2**, 161–166 (2009).
- 23 32. Fan, X. *et al.* Atomic arrangement of iodine atoms inside single-walled carbon  
24 nanotube. *Phys. Rev. Lett.* **84**, 4621–4624 (2000).
- 25 33. Gunlycke, D., Li, J., Mintmire, J. W. & White, C. T. Edges bring new dimension  
26 to grapheme nanoribbons. *Nano Lett.* **10**, 3638–3642 (2010).

## Acknowledgements

This work was supported by the DFG (German Research Foundation) and the Ministry of Science, Research and the Arts (MWK) of Baden-Württemberg in the frame of the SALVE (Sub Angstrom Low-Voltage Electron microscopy project) and by the DFG within the research project SFB 569 (U.K. and J.B.); the EPSRC (Career Acceleration Fellowship), NanoTP COST action and High Performance Computing (HPC) facility at the University of Nottingham (E.B.); the EPSRC, ESF and the Royal Society (A.N.K. and A.C.); the FP7 Marie Curie Fellowship (M.C.G-L.); and the Nottingham Nanoscience and Nanotechnology Centre (access to Raman spectrometer).

## Author contributions

A.C. and J.B. carried out transmission electron microscopy experiments (Ulm University) and image analysis. E.B. and N.K. performed theoretical modelling. M.C.G-L. and T.W.C. synthesized materials. G.A.R. carried out Raman spectroscopy measurements. U.K. contributed to the development of the experimental methodology and the discussion of the results. A.N.K. proposed the chemical structure of nanoribbon and the pathway of its formation, and wrote the original manuscript. All authors discussed the results and commented on the manuscript.

## Additional information

The authors declare no competing financial interests. Supplementary information accompanies this paper on [www.nature.com/naturematerials](http://www.nature.com/naturematerials). Reprints and permissions information is available online at <http://www.nature.com/reprints>. Correspondence and requests for materials should be addressed to A.N.K.

*Query 1: Line no. 4*

Three cases of somewhat have been removed/replaced as the word is not allowed according to NPG style.

*Query 2: Line no. 97*

Refs 2 and 3. FYI 'grapheme' corrected to 'graphene'.

*Query 3: Line no. 139*

Please provide page/article number for ref. 20.